Impact of insulation and wall thickness in compressed earth buildings in hot and dry tropical regions

Ibrahim Neya, Daniel Yamegueu, Yézouma Coulibaly, Adamah Messan, Arnaud Louis Sountong-Noma Ouedraogo

Impact of insulation and wall thickness in compressed earth buildings in hot and dry tropical regions

Ibrahim Neya[1, 2], Daniel Yamegueu[1, *], Yézouma Coulibaly[1], Adamah Messan[2] and Arnaud Louis Sountong-Noma Ouedraogo[2]

[1]Laboratoire Énergie Renouvelable et Efficacité Energétique, Institut International d'Ingénierie de l'Eau et de l'Environnement, Ouagadougou, Burkina Faso.

[2]Laboratoire Eco-Matériaux et Habitat Durable, Institut International d'Ingénierie de l'Eau et de l'Environnement, Ouagadougou, Burkina Faso.

Abstract

Outdoor climatic conditions such as sun radiation, air temperature and humidity, wind speed are the main factors that determine the thermal response of free-running buildings. However, the thermal behaviour of buildings can be regulated by a proper choice of suitable materials to maintain thermal comfort for the occupants. Through a validated energy model, this article evaluates the influence of insulation and thermal mass on the envelope of a compressed stabilised earth blocks test cell in a hot and dry tropical climate. The study assesses the impact of these parameters on building thermal performance. The effect of insulation is studied by considering different insulators made of glass wool or straw mixed with lime. The thermal inertia impact has been assessed by varying the wall thickness. The results show that insulation with 0.10 m glass wool thickness and 0.15 m straw mixed with 0.02 m lime have very close thermal performance. The study also shows that the appropriate wall thickness for adequate thermal comfort depends on the building insulation state. Without insulation, the wall thicknesses of 0.22 m and 0.35 m showed the best thermal performance. The corresponding decrement factors were respectively 30% and 17%. An insulated wall thickness of 0.14 m was

* Corresponding author. Phone: +226 68 76 87 65 – Email address: daniel.yamegueu@2ie-edu.org

the optimal choice because this choice lowered outdoor temperature amplitude to 22% and was more resource efficient.

Keywords: thermal behaviour, tropical climate, energy model, experimental validation, thermal comfort.

1. Introduction

The rapid growth of African population combined with a high urbanisation rate increase the need for decent dwellings with satisfactory comfort conditions for occupants [1]. In warms regions, cooling needs are especially high to adapt to current hot conditions. Therefore there is a real interest in low energy consumption houses in these regions where air conditioners ownership is around 0.06 units per household [2]. In Africa, people use widely ecological low-cost building materials such as earth, wood, straw and bamboo. However, the potential of these materials to time-shift and dampen the peak thermal loads have not been sufficiently investigated. This phenomenon known as thermal inertia effect characterises the building ability to store the daytime heat and release it in nighttime. The impact of the building envelope thermal inertia consists in providing a 'passive thermoregulation cooling' [3]. This leads in improving the building indoor thermal conditions without any energy consumption.

Verbeke and Audenaert [4] highlighted the discrepancies of thermal inertia effect in terms of cooling and heating loads reduction. The low indoor temperature observed in medieval churches show the practical benefits of thermal inertia. Some studies on dwellings made of earth [5], stone [6] and concrete [7] proved that thermal inertia ensure the thermal stability of building indoor environment. Contrary to this general observation, some authors pointed out that the net cooling demand of air conditioned buildings increases with thermal inertia in warms regions. This was noticed for example in the mediterranean climate of Italy [8] and hot desert climate of Las Vegas, USA [9]. In fact, in air-conditioned buildings, energy is required to cool down the additional thermal mass related to thermal inertia. The methods used in the different

studies, the scope of these studies and the buildings type explain partially the discrepancies found in the thermal inertia impact. However, thermal inertia is not the only phenomenon which determines buildings thermal behaviour. Other parameters such as building location and environment, its occupation scenario and insulation influence also the building thermal response [10].

To distinguish the building thermal inertia impact from other influencing parameters', some authors [3,11] used a numerical approach (theoretical models and simulations). Guglielmini et al. [3] analysed the influence of the thermal capacity of the peripheral walls and the indoor structures on thermal comfort. They found that insulation with glass wool of an external concrete wall influence the thermal inertia effect depending on the insulation layer position. However, this approach may face a gap between simulation and real performance.

Experimental approach can overcome this issue and provide accurate quantification of building thermal inertia. Brambilla and Jusselme [12] compared low and high thermal inertia constructions in the Swiss continental climate through experiments. The indoor temperature fluctuates less in the building with high thermal inertia, which improved indoor thermal stability. The indoor temperature was also up to 3 °C less in the higher thermal inertia building. However, the experimental methodology remains tedious and requires a lot of time, money and expertise to analyse all the different scenarios affecting the impact of thermal inertia. It is also difficult to distinguish with acceptable accuracy the thermal inertia effect from other influencing parameters impacts. Therefore a mix of simulation and experimental approaches could be a good compromise to analyse the thermal inertia effect.

The combination of these two methods is well known as empirical validation, and consists firstly in comparing measured and simulated data through building energy programs to assess the model ability to reproduce the building thermal behaviour. Secondly, when the numerical model precision is acceptable, the sensitivity analysis is performed and the influence of

77 different parameters involved is found with acceptable accuracy. Toure et al. [13] investigated
78 the influence of envelope thickness and solar absorptivity on time lag and decrement factor
79 using this approach. They found that increasing wall thickness improve the thermal inertia
80 effects as decrement factor and time lag. The study was performed in a test cell of $1m^3$ made
81 of compressed earth bricks stabilised with cement. The small size of the cell reduced the
82 influence of the complex physical heat exchange phenomena as conduction and radiation heat
83 gains through windows.
84 The present study aims to use the empirical validation approach to investigate the influence of
85 thermal insulation and thermal mass on full-scale building thermal inertia. The novelty of this
86 research stands in using local available materials such as compressed stabilised earth blocks
87 and straw to reduce overheating in dwellings.
88 Some previous studies pointed out the good performance of compressed earth blocks to offer
89 better durability than adobe materials [14,15] and offer same or better thermal response than
90 concrete in warms regions [14,16–18]. Other works [19–23] highlighted the benefits of using
91 straw in building construction. These materials are attractive alternatives to concrete and
92 conventional insulators which are usually more expensive and less ecologically friendly.
93 Tiskatine et al. [24] investigated thermal performance of cement stabilised red clays regarding
94 incorporation of insulators like sawdust, petiole, straw, argan shells, and palm fibres. They
95 found that the best thermal insulation performance is achieved with straw. Pritchard and Pitts
96 [20] presented straw as an abundant, ecological, inexpensive good thermal and sound insulator
97 even though like each material, it has some drawbacks. Quagliarini and Lenci [25] examined
98 the influence of straw as natural binder used in ancient adobe bricks of Roman and concluded
99 that straw influences both plasticity, breaking and shrinkage of adobe blocks. Aouba et al. [26]
100 showed that incorporating wheat straw in fired clay bricks reduce their thermal conductivity
101 by 35%.

The case study facility is a free-running compressed earth test cell built in a hot and dry tropical climate country. First, the study proposes experiments of the test building. Then, the energy model of the building is validated through an empirical validation approach. The passive strategies are thus examined using the validated numeric model of the building. Finally, the results are discussed and some recommendations are made.

2. Methodology

2.1 Description of the building

The experimental platform is located on the site of the International Institute for Water and Environmental Engineering (2iE) in Burkina Faso (12.5 ° north, 1.5 ° west). A test building was built on this site, with 0.14 m thick Compressed Stabilised Earth Brick (CEB) walls. This material results from the stabilisation of laterite, a local abundant material mixed with 8% of cement Portland CEMII. The use of cement improves the durability and mechanical strength of this earth-based material. Fig. 1 shows the test cell and its architectural plans. The test cell is a 3.06 m wide, 4.06 m long and 4.33 m high building. The size is representative of most buildings used by low-income population in rural and suburban areas of the country.

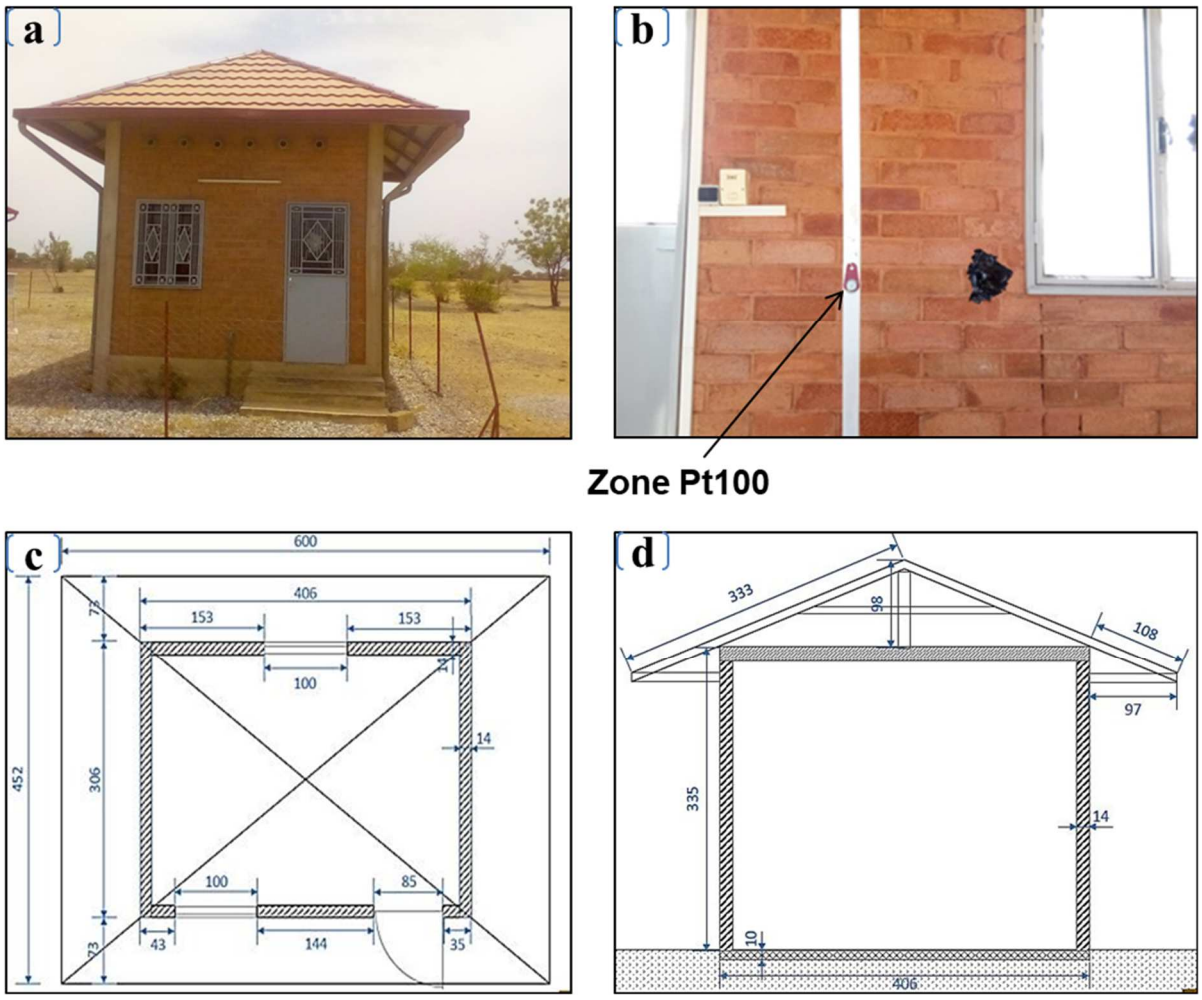

Fig. 1. (a) Test cell front view (b) monitoring sensor (c) top view and (d) front view

A recent study conducted by Rincón et al. [27] in this location used an adobe building of similar size to assess thermal comfort in earthen buildings. Other authors used similar test cells to investigate thermal performance of building in locations such as Mexico [28], France [29] and Switzerland [30]. Their work showed that test cells represent practical and efficient means to gather high quality data for empirical validation. They are a good compromise between laboratory and large-scale building experiments [31].

The test cell building considered in the present study is oriented east – west with two identical 3 mm single glazing windows of 1.00 m wide and 1.20 m high. The windows are located on the north and south facades. The door of 0.85 m wide and 2.20 m high is made of metal and glazing identical to the windows in its upper part. It is on the south facade. The floor is a 0.10 m

130 concrete slab. The roof of the test building is of 1.5 mm metal sheet. This is the most used roof
131 material in low-income communities. The roof benefits from natural ventilation through five
132 openings of 0.10 m diameter on the main facades. The ceiling is made of 5 mm plywood.

133 The thermophysical properties of the materials used for the building envelope are given in
134 Table 1.

135 **Table 1.** Thermophysical properties of building materials

	conductivity ($W\ m^{-1}\ K^{-1}$)	**density ($kg\ m^{-3}$)**	**specific heat ($J\ Kg^{-1}\ K^{-1}$)**
CEB	1.02	986	1,935
Concrete	1.4	2,240	840
Wood	0.15	1,200	500
Metal sheet	50	7,800	480
Glass wool	0.04	200	1.21
Straw	0.06	100	1,700
Lime	1.2	1,600	1,000

136

137 The model also includes the windows and other openings thermal gain calculation. To do so,
138 their materials thermal properties were taken from the EnergyPlus database. To characterise
139 the thermal response of the test cell regarding outdoor climatic conditions, the building was
140 kept closed and in free-running mode during the experiments.

141 **2.2 Data Collection**

142 The temperature was recorded using a Pt 100 of range -20 °C to 85 °C with an accuracy of
143 0.12 °C. The sensor was set at a height of 1.1 m from the ground in the centre of the room. The
144 outdoor weather parameters of the study site were recorded using a Vaisala HydroMet weather
145 station located on the experimental site (**Fig. 2**). The measured parameters are the dry
146 temperature, the relative humidity, the global solar irradiation, the diffuse solar irradiation, the
147 wind speed and direction.

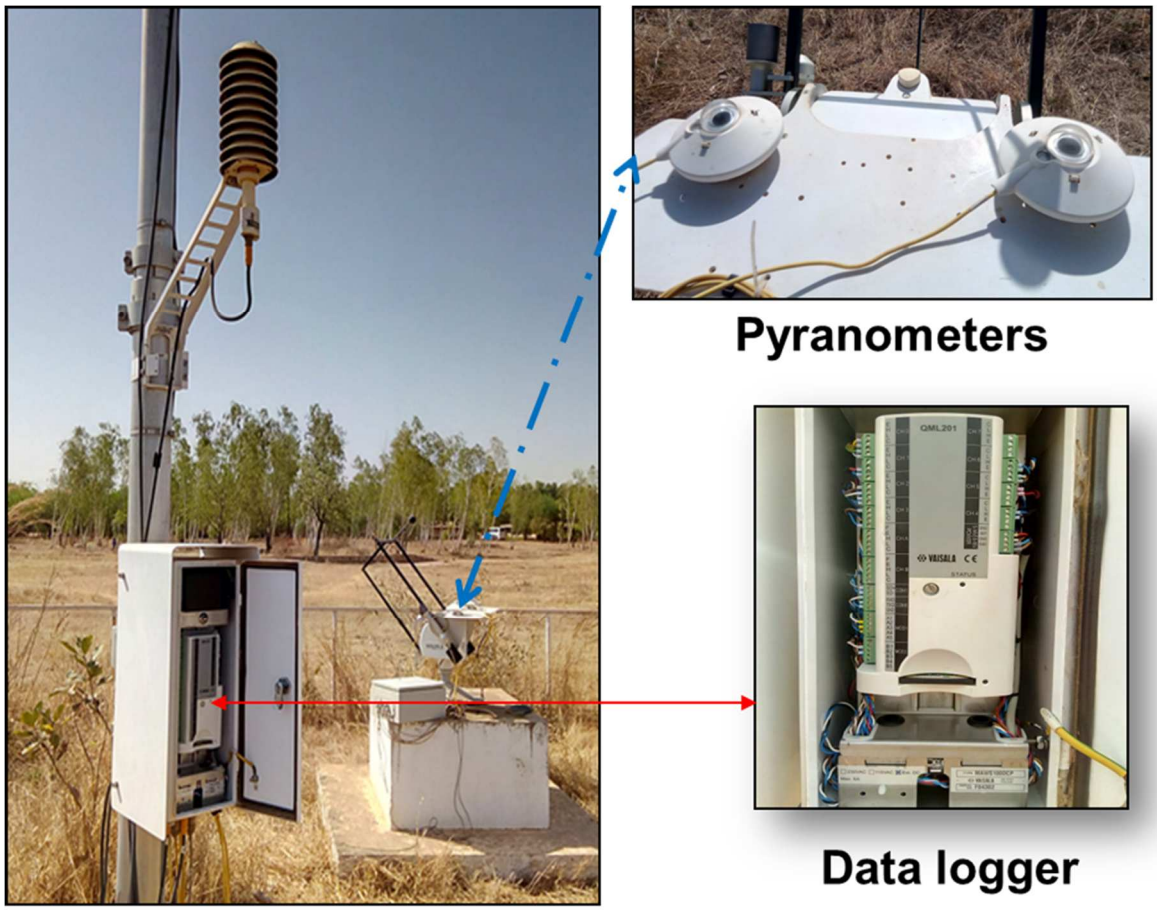

Fig. 2. Weather station located on the experimental building platform

3. Modelling and simulation of the building

3.1 Model development

The model was implemented in the dynamic simulation engine EnergyPlus 9.0.1, released in October 2018. EnergyPlus is one of the most advanced and most used energy-simulation programs. EnergyPlus is commonly used to model and analyse the dynamic thermal behaviour related to energy and provides accurate temperature and comfort prediction [32–35].

The thermal conduction of the model is evaluated with the Conduction Transfer Functions (CTF) recommended in [36] for the hot and dry climate. Considering the CTF model, the heat flux at one surface is linearly related to the prevalent and some of the past temperatures at both the interior and exterior surface as well as some of the past flux values at the other surface as shown by the Eq. 1–2 [37]. The CTF is solved in EnergyPlus using the basic state space method

with finite difference variables as described in [37]. In the resolution using Conduction Transfer Functions method, nz and nq are respectively the number of CTF temperature and flux coefficients. They are constant and depend on the construction type.

$$q''_{ki}(t) = -Z_o T_{i,t} - \sum_{j=1}^{nz} Z_j T_{i,t-j\delta} + Y_o T_{o,t} + \sum_{j=1}^{nz} Y_j T_{o,t-j\delta} + \sum_{j=1}^{nq} \Phi_j \, q''_{ki,t-j\delta} \quad (1)$$

$$q''_{ko}(t) = -Y_o T_{i,t} - \sum_{j=1}^{nz} Y_j T_{i,t-j\delta} + X_o T_{o,t} + \sum_{j=1}^{nz} X_j T_{o,t-j\delta} + \sum_{j=1}^{nq} \Phi_j \, q''_{kO,t-j\delta} \quad (2)$$

With:

X_j, the outdoor CTF coefficient

Y_j, the cross CTF coefficient

Z_j, the indoor CTF coefficient

Φ_j, the flux CTF coefficient

T_i, the indoor face temperature

T_o, the outdoor face temperature

q''_{ko} = Conduction heat flux on outdoor face

q''_{ki} = Conduction heat flux on indoor face

The subscript following the comma indicates the time period for the quantity in terms of the time step δ.

The Thermal Analysis Research Program from ASHRAE is used for both external and internal convective heat exchange [37,38]. Outdoor global coefficient (Eq. 3) is split into forced component and natural component, respectively evaluated in Eq. 4 and Eq.5. Indoor convective coefficient is calculated here using natural convection equation (Eq.5).

$$h_c = h_f + h_n \quad (3)$$

Where hc, hf and hn are respectively global convective, forced convective and natural convective coefficients.

$$h_f = 2.537\, W_f R_f \left(\frac{PV_z}{A}\right)^{1/2} \quad (4)$$

Where:

Wf is the wind direction multiplier,

Vz is the wind speed at height above ground of the surface centroid,

A is the surface area of the surface

P is the perimeter of the surface

Rf is the surface roughness multiplier

For natural convection:

- When ΔT = 0 or a vertical surface

$$h_n = 1.31\, |\Delta T|^{\frac{1}{3}} \quad (5.1)$$

- For (ΔT < 0.0 on an upward facing surface) or (ΔT > 0.0 on a downward facing surface

$$h_n = \frac{9.482\, |\Delta T|^{\frac{1}{3}}}{7.283 - |cos\ \Sigma|} \quad (5.2)$$

- For (ΔT > 0.0 on an upward facing surface) or (ΔT < 0.0 on a downward facing surface

$$h_n = \frac{1.810\, |\Delta T|^{\frac{1}{3}}}{1.382 + |cos\ \Sigma|} \quad (5.3)$$

With:

ΔT, the temperature difference between the surface and air

Σ, the surface tilt angle

Air infiltration was evaluated using the model of effective leakage area [39]. The infiltration was assessed according to that handbook method as mentioned in Eq.6:

$$Infiltration = (F_{schedule})\frac{A_L}{1000}\sqrt{C_s\Delta T + C_w(WindSpeed)^2} \quad (6)$$

Where:

Fschedule is a value from a user-defined schedule,

AL is the effective air leakage area in cm2

Cs is the coefficient for stack-induced infiltration

ΔT is the absolute temperature difference between zone air and outdoor air,

Cw is the coefficient for wind-induced infiltration

WindSpeed is the local wind speed.

3.2 Thermal Model Validation

The empirical validation of the model consists in comparing the temperatures predicted (T_{sim}) by the model with the measured ones (T_{meas}) in the test cell. Two main statistical indicators for model validation are used. The first one is the average absolute difference between measured and simulated data [40] (Eq. 7). The second one is the linear correlation coefficient R^2 (Eq. 8). In Eq. 3–4, the indices i refer to single record and n to the total number of records.

$$Avg.\,abs.\,error\ (°C) = \frac{\sum_{i=1}^{n}\left|T_{sim,i} - T_{meas,i}\right|}{n} \quad (7)$$

$$R^2 = 1 - \frac{\sum_{i=1}^{n}\left(T_{sim,i} - T_{meas,i}\right)^2}{\sum_{i=1}^{n}\left(T_{meas,i} - \overline{T_{meas,i}}\right)^2} \quad (8)$$

3.3 Inertia and insulation effect on buildings

The building envelope thermal inertia and insulation characterise the envelope capacity to regulate indoor climate by dampening and shifting outdoor thermal loads. Two main regulation

effects are commonly used to assess the building performance in this regard. These are the time lag and the decrement factor. The two indicators are evaluated between the outdoor and indoor ambiance temperatures as mentioned in [41].

The decrement factor is calculated as the temperature amplitudes ratio between their indoor values and outdoor values (Eq. 9). The decrement factor express the building potential to dampen the heat flux transfer due to external thermal solicitations as solar radiation and outdoor temperature.

The time lag expresses how long it takes to the outdoor temperature to reach the interior of the building (Eq. 10). The thermal time lag expresses the building capacity to delay the thermal loads impact on indoor temperature to keep the building cool in warms periods.

$$f = \frac{T_{i,max} - T_{i,min}}{T_{o,max} - T_{o,min}} \quad (9)$$

With T: temperature, i: indoor, o: outdoor, max: maximum, min: minimum and t: time

$$\emptyset = t_{T_{i,max}} - t_{T_{o,max}} \quad (10)$$

4. Empirical validation

4.1 Experimental results

Data considered for the analysis in the present study are those for April, the hottest month of the country and therefore the most uncomfortable. The monitoring was performed in the year 2018. For illustrative purpose, all the following figures except Fig. 6 will cover only the first week of April as the representation of the whole month may hide some gaps between data. However, the data analysis and discussion cover the whole month of April to draw conclusions representative of the overheating reduction of the alternatives considered.

The experiments were achieved during clear sky conditions and absence of precipitations. The daily peak irradiance values are between 850 W·m^{-2} and 1120 W·m^{-2}. They are observed at

12 AM and 1 PM respectively. Globally, the irradiance values are above 100 $W \cdot m^{-2}$ between 8 AM to 5 PM.

Fig. 3 presents a weekly time evolution of relative humidity and outdoor temperature. One can notice that the outdoor temperature fluctuates between 24 °C and 41 °C with a mean value of 33 °C while relative humidity varies between 6% and 70%. The outdoor air temperature maximum is observed around 3–5 PM and the minimum around 6–7 AM. During the daytime, outdoor temperature increases while relative humidity decreases. In night-time, outdoor temperature decreases while relative humidity increases.

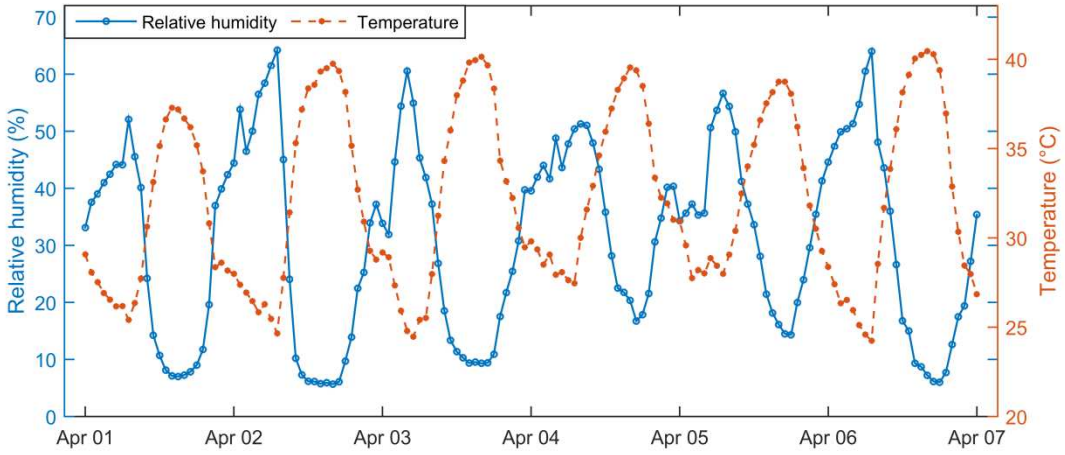

Fig. 3. Weekly temperature and humidity from the weather station

Fig. 4 compares indoor and outdoor measured temperatures. The measured indoor temperature varies between 29 °C and 42 °C with a mean value of 36 °C. The indoor temperature maximum occurs between 5 PM and 6 PM, and the minimum between 7 AM and 8 AM. The outdoor and indoor temperatures are closer during the daytime than nighttime. The differences between maximum outdoor and indoor temperatures are smaller than gaps between minimum indoor and outdoor temperatures.

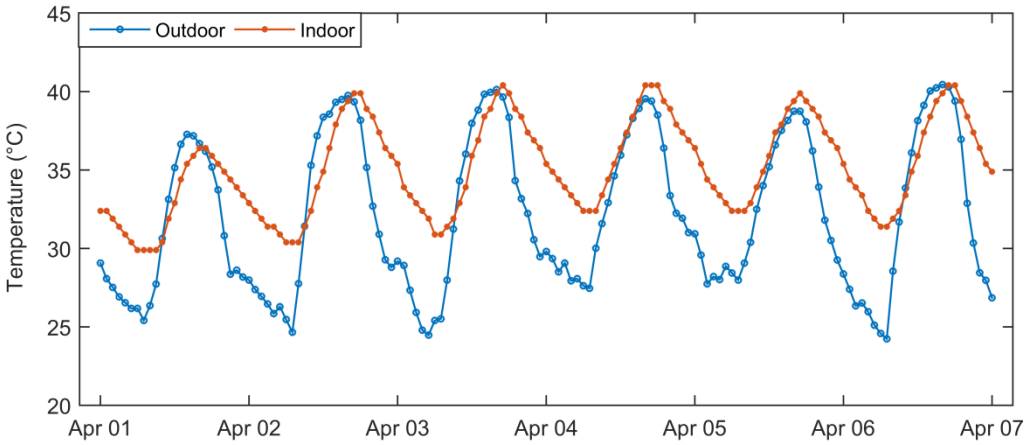

Fig. 4. Weekly outdoor and indoor temperatures

The quick rise of indoor temperature with outdoor temperature during the daytime is probably due to the high solar radiation. Therefore it is suitable to limit heat transfer from outdoor to indoor ambiance using insulation. It is also possible to increase the envelope thermal mass to absorb the solar gains received from the walls, openings and the roof. The absence of solar radiation during nighttime explains the low difference between indoor and outdoor temperature extrema. The natural ventilation during nighttime can accelerate the building cooling process because of the fresh outdoor nighttime temperature.

4.2 Model results and empirical validation

The measured and simulated buildings indoor temperatures are plotted in Fig. 5.

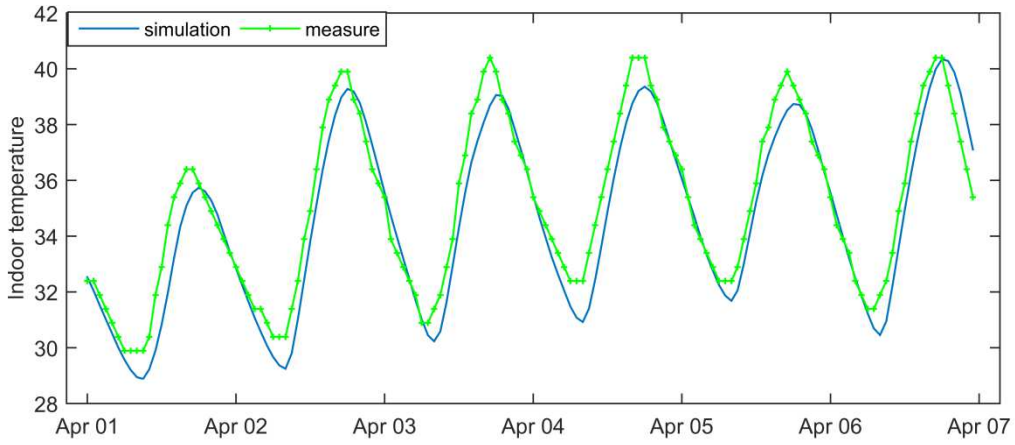

Fig. 5. Measured and simulated temperature of building indoor environment

The temperature measurement uncertainty was 0.12 °C. This uncertainty is too small to be visible on the graph and was not drawn. The measured temperature varies between 29 °C and 42 °C and the simulated ones between 28 °C and 43 °C. A fairly good agreement can be observed between model and experiment. A good linear relationship is observed between simulated and measured temperature with residues less than 2 °C (Fig. 6). The calculated mean absolute error value is 0.76 °C and the correlation coefficient is equal to 0.93.

The absolute mean difference is between 0.5 °C and 1 °C. This range is reasonable because of the measurement and calculation uncertainties [42]. The discrepancies could be explained by the uncertainties related to material properties taken in the literature. The R^2 value shows a strong fit between simulated and measured temperatures. Thus the building thermal model is acceptable for simulation cases assessment.

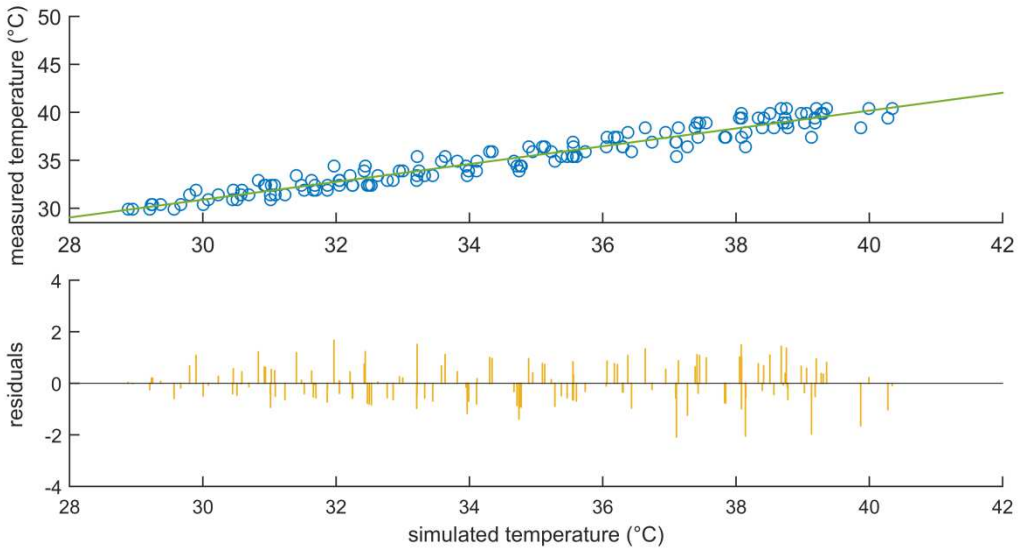

Fig. 6. Fitting between measured and simulated data

5. Simulation case studies

5.1 Simulation scenarios

The aim of this modelling is to set up a tool to help in the thermal design of houses in warms regions by assessing how indoor temperature can be reduced using various architectural effects and local building materials.

Building indoor temperature is a prerequisite parameter to assess the thermal comfort in free-running mode. The following case studies intend to study the effect of wall insulation and block thickness on the indoor temperature of test cells. The two proposed options were combined in the last section in order to assess their combined effect on indoor temperature of test cells.

To assess the typical performance of the test cell, the climatic data of the Station 655,030 (N 12° 21', W 1° 31'; 316 m above sea level) of Ouagadougou, representative of long-term period, were used. During the hottest month, April, dry bulb temperatures fluctuate in range 23–43 °C; and relative humidity in range 15–80 %. The global horizontal irradiation varies between 1053 $W.m^{-2}$ during the same period. The maxima of temperature and global solar irradiation are observed respectively during 1–2 PM and 11 AM-1 PM. The baseline simulation case corresponds to the initial building model simulated with the climatic data file.

5.2 Influence of Insulation on the Cell Indoor Temperature

The insulation analysis aims in this case to compare the traditional glass wool material with the innovative use of a mixture made of lime and straw. The different insulation simulation cases are shown in Fig.7. They are used to insulate the outdoor surface of walls and thus protect the indoor environment from the solar radiation and outdoor ambient air gains.

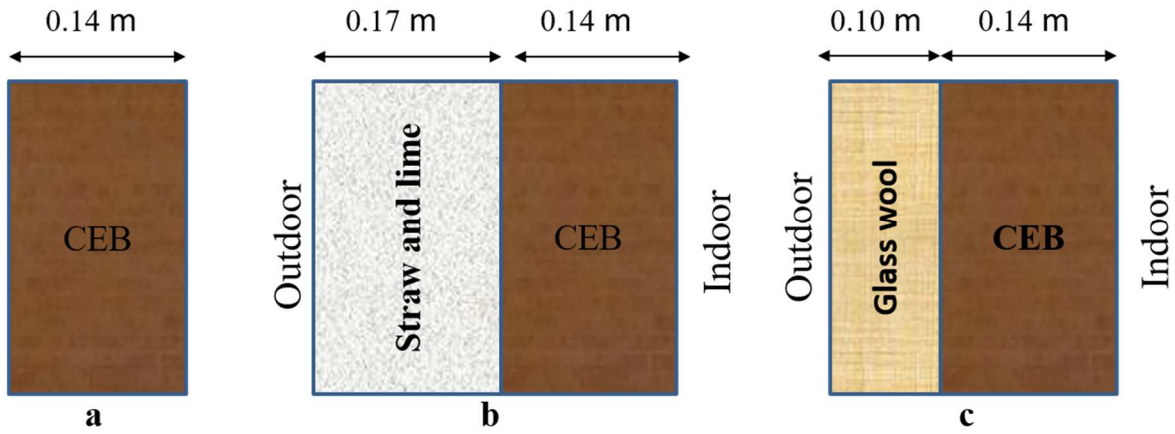

Fig.7. Insulation simulations (a) baseline case (b) CEB with straw and lime mixture (c) CEB with glass wool

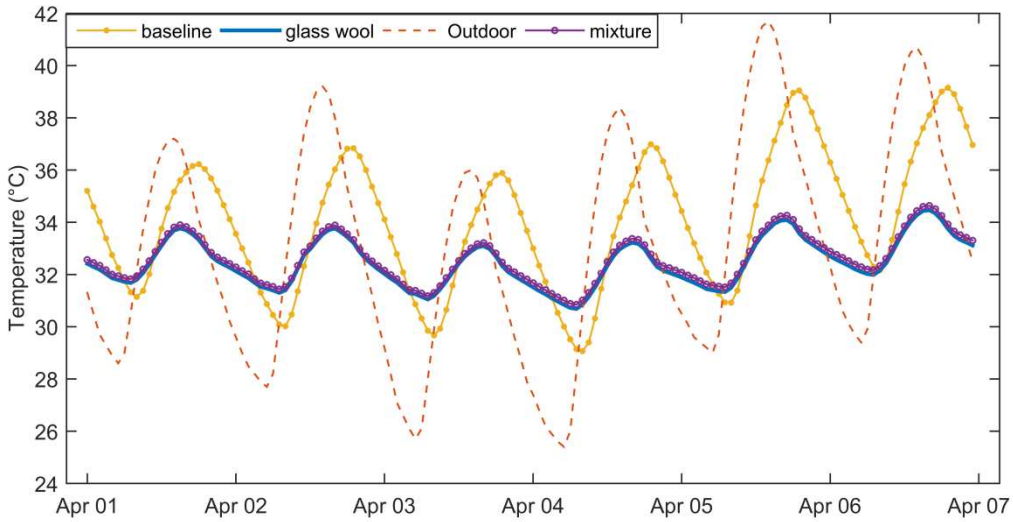

Fig. 8. Influence of glass wool and straw insulation on the external surface of walls

The materials disposition ensures that the CEB is in contact with the building indoor environment. Such disposition improve the building thermal performance in all climate zones[10]. The glass wool thickness considered was 0.10 m and the mixture was 0.15 m of straw recovered with 0.02 m of lime. The thermophysical properties of these materials are given in Table 1.

Fig. 8 shows the simulation results of the two proposed insulation solutions. The results are compared to the baseline case without any insulation.

One can see that the two insulation cases have close thermal performance. Compared to the reference case, the use of insulation provides interesting indoor temperature reduction. The

value of decrement factor in the baseline case, 0.61 decreases to 0.22 in the insulation cases. The insulation therefore reduces the decrement factor by 64%. However, the time lag is reduced of 2.50 from baseline to insulation cases.

The outdoor temperature ranges between 23 °C and 43 °C. The indoor temperature varies between 27 °C and 41 °C for reference case; and 29 °C and 36 °C for insulation cases. The maximum daily daytime temperature reduction between insulation and reference case fluctuates between 2 °C and 6 °C. The mean daytime temperature reduction is evaluated at 2 °C. During nighttime, temperature in the reference case is lower than those of insulation cases. The mean temperature gain is 0.8 °C with a maximum value of 2.8 °C.

5.3 Influence of Wall Thickness on the Cell Indoor Temperature

The second option considered consists in using blocks of different thicknesses to assess their capacity to store the heat and thus better regulate the indoor thermal conditions. The 0.14 m and 0.22 m thicknesses are the commonly used thicknesses for compressed earth blocks in the country. The thickness of 0.35 m and 0.50 m are also used to further investigate the influence of wall thickness. The different simulation cases on wall thickness are shown in Fig. 9.

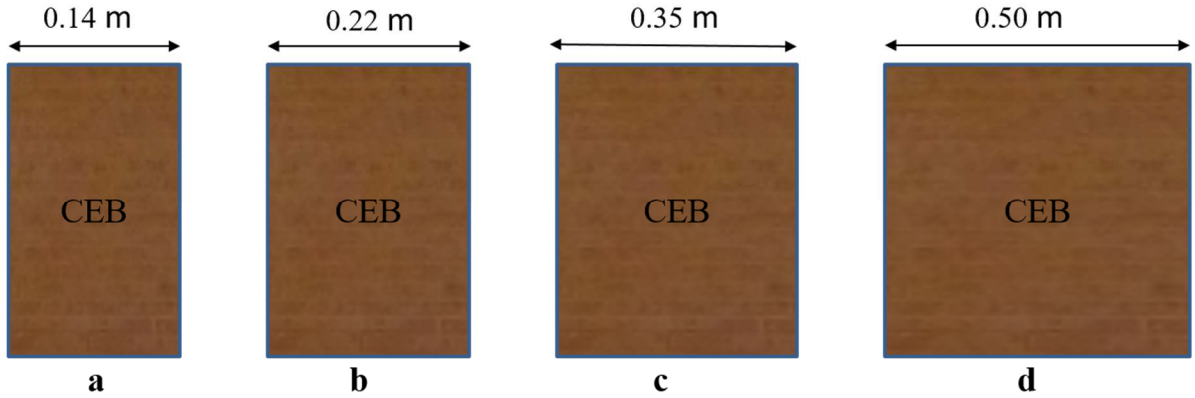

Fig. 9. Simulation cases of wall thicknesses (a) 0.14 m CEB (b) 0.22 m CEB (c) 0.35 m CEB (d) 0.50 m CEB

The mean indoor temperature fluctuates around 34 °C with progressive reduction in amplitude up to thickness 0.35 m. The simulation shows how the block thickness influences the indoor temperature. In fact, increasing thickness reduces the indoor temperature amplitudes (Fig. 10).

335 Compared to the baseline where the block thickness is 0.14 m, the daytime temperature
336 reduction reaches 3 °C, 5 °C and 5 °C respectively for thickness 0.22 m, 0.35 m and 0.50 m.
337 The mean values of these reductions are 1.0 °C, 1.6 °C and 1.7 °C. During nighttime, the
338 temperature in the baseline case is the lowest. The mean temperature gains are 0.9 °C, 1.2 °C
339 and 1.3 °C respectively for 0.22 m thickness, 0.35 m and 0.50 m. One can notice that the results
340 for 0.35 m and 0.50 m are close. This means that there is no interest to consider thickness more
341 than 0.35 m for the case study. Table 2 shows temperature, decrement factor and time lag
342 ranges and their mean values.

343 **Table 2.** Thermal performance of test cell for different wall thickness

	CEB 0.14 m	CEB 0.22 m	CEB 0.35 m	CEB 0.50 m
Temperatures				
Range (°C)	27–41	29–39	30–37	30–37
Mean (°C)	34.0	33.9	33.7	33.5
Decrement factor	0.61	0.30	0.17	0.21
Time lag (h)	4.50	4.63	2.00	1.50

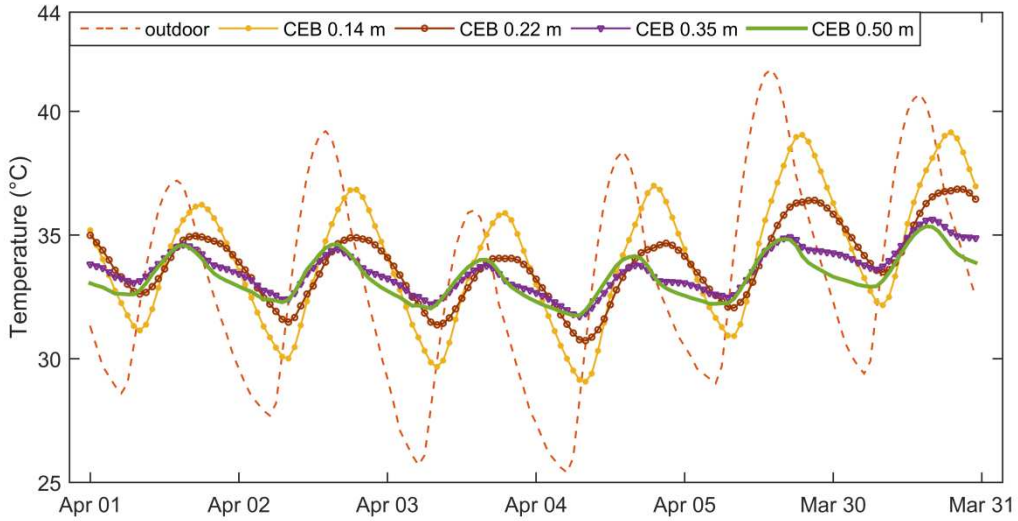

344

345 **Fig. 10.** Influence of blocks thickness on the building thermal response

346 **5.4 Combined influence of insulation and blocks thickness**

347 The earlier sections study the separate effects of the insulation and thermal mass on building
348 indoor temperature variation. They were found useful to dampen thermal waves of outdoor

environment. This section aims to assess the combined effect of the two previous options on the building indoor temperature. As shown by the results obtained in the previous sections, insulation with 0.10 m of glass or 0.15 m of straw mixed with 0.02 m of lime have similar thermal performance. Hence, only the mixture of straw and lime is used for the following simulations. Therefore, the variation of indoor temperature is analysed through different wall thickness recovered with the same mixture of lime and straw (Fig. 11).

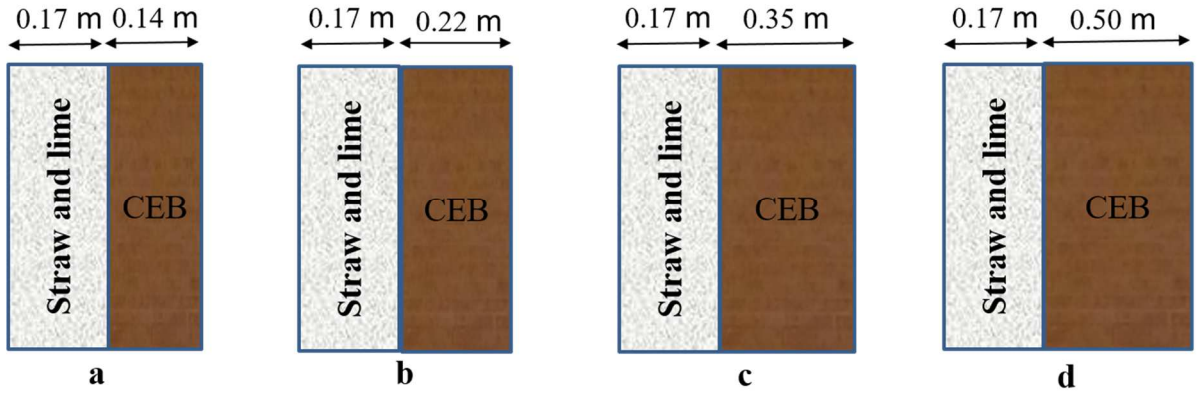

Fig. 11. Simulation cases of CEB with outside side straw and lime insulation of thicknesses (a) 0.14 m (b) 0.22 m (c) 0.35 m and (d) 0.50 m

Table 3 summarises the statistical parameters as function of the blocks thickness.

Table 3. Thermal performance of insulated test cell according to wall thickness

	CEB 0.14 m	CEB 0.22 m	CEB 0.35 m	CEB 0.50 m
Temperatures				
Range (°C)	29° C-36°C	30° C-36°C	30° C-36°C	30° C-36°C
Mean (°C)	32.7 °C	32.7 °C	32.7 °C	32.6 °C
Decrement factor	0.22	0.22	0.23	0.24
Time lag (h)	1.90	1.80	1.80	1.70

The indoor temperature for the different cases of blocks thickness ranges between 29 °C and 36 °C with decrement factor around 0.23 and a time lag of 1.80 h.

The indoor temperatures are very close for the different blocks thicknesses (**Fig. 12**).

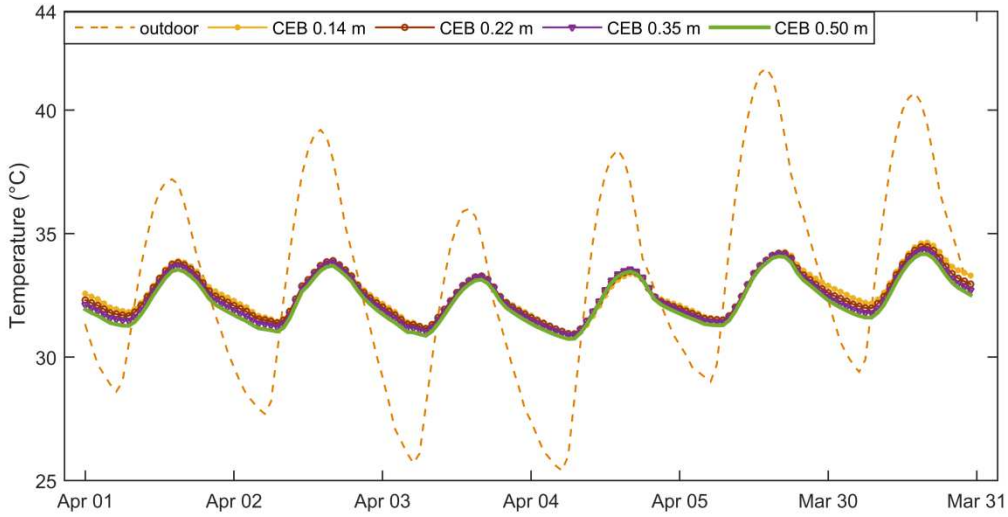

Fig. 12. Combined influence of insulation and wall thickness on indoor temperature

5.5 Simulation discussions

Here the time lag was expected to increase with insulation as referenced in [43]. Such results were found only for CEB 0.14 m and CEB 0.20 m where time lag increase a little with values between 4-5 h. However for other simulation cases, time lag values were less than 2 h. In fact, the more the thermal mass or insulation thickness, the less the heat conduction through the building wall. As mentioned [13] beyond 32 cm, the indoor environment is no longer influenced by the outdoor thermal flux through walls. This explains why the effect of thermal mass on thermal lag is more pronounced for thicknesses 0.14 m and 0.22 m; and not 0.35 m and 0.50 m. Because insulation and CEB 0.35 m and CEB 0.50m hinder heat conduction through walls, the low values of thermal lag obtained are related to direct daytime heat gains through the building's other components, especially openings and roof. In fact, the building air because of its low heat capacity is influenced by these heat gains and the indoor temperature keeps increasing until sunset. The maximum indoor temperature is thus reached and the building cooling begins through thermal radiation and convection heat exchanges. But in the CEB 0.14 m and CEB 0.22 m in thermal mass influence, because the walls have stored more

energy during the daytime, they continue to increase the building indoor temperature until they reached equilibrium with the outside environment.

Insulation impact analysis shows that insulation lowers indoor temperature during the daytime. In fact, insulation with the mixture of 0.15 m straw and 0.02 m lime or glass wool reduce the building indoor temperature up to 6 °C. In the nighttime, natural ventilation can cancel the reverse effects of insulation and provide better comfort conditions using outdoor fresh air. Insulation also ensures better thermal stability. In fact, insulation reduces by two third the decrement factor when compared to the baseline scenario. This is mainly due to the insulation capacity to reduce the heat transfer through walls in the building indoor environment. Time lag of 2 h may be seen not enough, meaning that adequate thermal inertia is not obtained. Nonetheless, insulation remains a very attractive solution as the low indoor temperature amplitude makes the heat exchange time less important.

For the wall inertia assessment, the higher the wall thickness, the lower the indoor temperature. The decrement factor and time lag of CEB 0.14 m (Table 2), respectively of 0.61 and 4.50 h are low for adequate thermal inertia when compared to values of 6 hours of time lag and 0.40 of decrement factor for sufficient thermal inertia [44]. Toure et al. [43] found time lag values in the range 6.02 h - 6.38 h and decrement factor in the range 0.38-0.43 by experimental analysis for a 1x1x1 m^3 test cell of 14 cm stabilised earth blocks with cement. The discrepancies with the present results may be mainly due to the test cell scale, difference in CEB thermophysical properties and air humidity that can impact the thermal properties. In fact, the CEB properties are dependent on the laterite properties that also depend on the quarry. The investigation of Asan and Sancaktar 1998 showed that thermal inertia effects depend on material thermal properties. Concerning air humidity, the study was achieved in the humid climate of Senegal as opposed to the dry climate of our case. Indeed, Shaik et al. [46] proved that ambient relative humidity, temperature and outdoor convection coefficient influence

410 greatly the decrement factor and time lag of laterite material. As earth material is sensitive to
411 water, this affects the thermal performance of buildings. Because of the good thermal stability
412 obtained with CEB 0.22 m, CEB 0.35 m and CEB 0.50 m, they can be used to improve indoor
413 thermal comfort. When block thickness is increased by 57% from CEB 0.14 m to get
414 CEB 0.22 m, by 150% to get CEB 0.35 m, and by 257% to get CEB 0.50 m, the mean indoor
415 temperature reduction is respectively 1.0 °C, 1.6 °C and 1.7 °C. Therefore the thickness of
416 0.50 m is less attractive because of the higher mass increase with less thermal impact. Further
417 investigations on economic and environmental issues are also suitable for optimal choice of
418 blocks thickness.

419 Concerning the combination of the alternatives, for the different blocks thickness, the indoor
420 temperature amplitude is about 6 °C. A good indoor thermal stability is observed with daily
421 values of decrement factor below 0.30. The time lag values are very close. Because all the cases
422 of wall thickness simulated offer slightly the same thermal performance, the insulation effect
423 is dominant on the thermal mass impact. An optimal insulation layer can thus be investigated
424 to take advantage of both thermal mass and insulation potential of the blocks thickness. Yet,
425 because it requires the least material quantities, the CEB 0.14 m is the most advantageous when
426 using typical insulation and material thicknesses. The different simulation scenarios show how
427 insulation and thermal mass of building envelope walls influence the building thermal
428 behaviour. Furthermore, improving indoor climatic conditions through dwelling envelope
429 thermal enhancement is still possible by reducing the heat transmission through the building
430 openings and roof; and also using nocturnal natural ventilation. Another investigation that
431 could be addressed in future works concerns the possibility of storing the night freshness in
432 building internal partitions to improve the cooling down of the whole structure.

6. Conclusion

The study aims to assess the thermal impact of the thermal inertia and insulation of a free-running Compressed Earth Brick (CEB) test building. A building model was built on the leading software EnergyPlus and validated through multiple adequate statistical indicators that demonstrate the ability of the model to reproduce with acceptable accuracy the thermal behaviour of the building. Hence, simulation was performed to investigate the building wall capacity to regulate the indoor thermal conditions regarding hot climatic external conditions. It is found on one hand that an insulation of walls with 0.10 m glass wool and a mixture of 0.02 m lime and 0.15 m straw give the same thermal performance, and, on the other hand, that wall thicknesses of 0.22 m and 0.35 m are acceptable in terms of performance, without any insulation. Results also show that a 0.14 m wall thickness is sufficient when an adequate insulation is used. The study contributes to fill the gap of information on the influence of earthen blocks thickness and insulation materials in harsh tropical climatic conditions. The use of straw, abundant in these regions, ecologically friendly and cheap, in contrast with glass wool, also contributes to the sustainable building approach. The practical thicknesses suggested are also important to avoid losing money on the basis that increasing wall thickness always augments building thermal inertial and therefore its comfort. The study weekly increase of temperatures in some experiments suggest that sequential inertia be part of this study. This will be one of the issues explored by the next study of the laboratory. Further investigation is underway and will provide in-depth insight on heat transmission reduction through openings and roof; and how passive strategies can be combined to ensure adequate thermal comfort conditions to low-cost houses in dry and hot climatic regions.

Acknowledgments

The authors acknowledge the support of the German Academic Exchange Office (DAAD) for funding the research that allowed this research work to be carried out.

Bibliography

[1] IEPF, Efficacité Énergétique de la climatisation en région tropicale, Institut de l'Énergie et de l'Environnement de la Francophonie, Québec, Canada, 2006. http://www.ifdd.francophonie.org/docs/prisme/eeTOME1.PDF.

[2] (International Energy Agency) IEA, Africa Energy Outlook: World Energy Outlook Special Report, IEA, Paris, 2019.

[3] G. Guglielmini, U. Magrini, E. Nannei, The Influence of the Thermal Inertia of Building Structures On Comfort and Energy Consumption, Journal of Thermal Insulation. 5 (1981) 59–72. https://doi.org/10.1177/109719638100500201.

[4] S. Verbeke, A. Audenaert, Thermal inertia in buildings: A review of impacts across climate and building use, Renewable and Sustainable Energy Reviews. 82 (2018) 2300–2318. https://doi.org/10.1016/j.rser.2017.08.083.

[5] K. Ip, A. Miller, Thermal behaviour of an earth-sheltered autonomous building – The Brighton Earthship, Renewable Energy. 34 (2009) 2037–2043. https://doi.org/10.1016/j.renene.2009.02.006.

[6] D. Medjelekh, L. Ulmet, S. Abdou, F. Dubois, A field study of thermal and hygric inertia and its effects on indoor thermal comfort: Characterization of travertine stone envelope, Building and Environment. 106 (2016) 57–77. https://doi.org/10.1016/j.buildenv.2016.06.010.

[7] B. Givoni, Effectiveness of mass and night ventilation in lowering the indoor daytime temperatures. Part I: 1993 experimental periods, Energy and Buildings. 28 (1998) 25–32. https://doi.org/10.1016/S0378-7788(97)00056-X.

[8] S. Ferrari, Building envelope and heat capacity: re-discovering the thermal mass for winter energy saving, (2007) 6.

[9] L. Zhu, R. Hurt, D. Correia, R. Boehm, Detailed energy saving performance analyses on thermal mass walls demonstrated in a zero energy house, Energy and Buildings. 41 (2009) 303–310. https://doi.org/10.1016/j.enbuild.2008.10.003.

[10] J. Jazaeri, R.L. Gordon, T. Alpcan, Influence of building envelopes, climates, and occupancy patterns on residential HVAC demand, Journal of Building Engineering. 22 (2019) 33–47. https://doi.org/10.1016/j.jobe.2018.11.011.

[11] L. Rodrigues, V. Sougkakis, M. Gillott, Investigating the potential of adding thermal mass to mitigate overheating in a super-insulated low-energy timber house, Int J Low-Carbon Tech. 11 (2016) 305–316. https://doi.org/10.1093/ijlct/ctv003.

[12] A. Brambilla, T. Jusselme, Preventing overheating in offices through thermal inertial properties of compressed earth bricks: A study on a real scale prototype, Energy and Buildings. 156 (2017) 281–292. https://doi.org/10.1016/j.enbuild.2017.09.070.

[13] P.M. Toure, Y. Dieye, P.M. Gueye, M. Faye, V. Sambou, Influence of envelope thickness and solar absorptivity of a test cell on time lag and decrement factor, Journal of Building Physics. (2019) 174425911986344. https://doi.org/10.1177/1744259119863446.

[14] O.B. Adegun, Y.M.D. Adedeji, Review of economic and environmental benefits of earthen materials for housing in Africa, Frontiers of Architectural Research. 6 (2017) 519–528. https://doi.org/10.1016/j.foar.2017.08.003.
[15] S. Omar Sore, A. Messan, E. Prud'homme, G. Escadeillas, F. Tsobnang, Stabilization of compressed earth blocks (CEBs) by geopolymer binder based on local materials from Burkina Faso, Construction and Building Materials. 165 (2018) 333–345. https://doi.org/10.1016/j.conbuildmat.2018.01.051.
[16] C. Yézouma, T. Godefroy, T.M. Yves, Climat et confort thermique, Sud Sciences & Technologies. 2 (1998) 6.
[17] Y. Jannot, T. Djiako, Economie d'énergie et confort thermique dans l'habitat en zone tropicale, Revue Internationale Du Froid. 17 (1994) 166–173. https://doi.org/10.1016/0140-7007(94)90015-9.
[18] C.M. Hema, G. Van Moeseke, A. Evrad, L. Courard, A. Messan, Vernacular housing practices in Burkina Faso: representative models of construction in Ouagadougou and walls hygrothermal efficiency, Energy Procedia. 122 (2017) 535–540. https://doi.org/10.1016/j.egypro.2017.07.398.
[19] D.Y.K. Toguyeni, Study of the influence of roof insulation involving local materials on cooling loads of houses built of clay and straw, Energy and Buildings. (2012) 7.
[20] M.B. Pritchard, A. Pitts, Evaluation of Strawbale Building: Benefits and Risks, Architectural Science Review. 49 (2006) 372–384. https://doi.org/10.3763/asre.2006.4949.
[21] D. Samuel, E. Arnaud, B. Christophe, L. Frédéric, Temperature and moisture storage in crop-based materials: Modelling a straw bale wall subject to a thermal shock, Journal of Building Physics. 39 (2016) 421–439. https://doi.org/10.1177/1744259115589680.
[22] O. Douzane, G. Promis, J.-M. Roucoult, A.-D. Tran Le, T. Langlet, Hygrothermal performance of a straw bale building: In situ and laboratory investigations, Journal of Building Engineering. 8 (2016) 91–98. https://doi.org/10.1016/j.jobe.2016.10.002.
[23] F. D'Alessandro, F. Bianchi, G. Baldinelli, A. Rotili, S. Schiavoni, Straw bale constructions: Laboratory, in field and numerical assessment of energy and environmental performance, Journal of Building Engineering. 11 (2017) 56–68. https://doi.org/10.1016/j.jobe.2017.03.012.
[24] R. Tiskatine, N. Bougdour, R. Oaddi, L. Gourdo, Y. Rahib, S. Bouzit, A. Bazgaou, L. Bouirden, A. Ihlal, A. Aharoune, Thermo-physical analysis of low-cost ecological composites for building construction, Journal of Building Engineering. 20 (2018) 762–775. https://doi.org/10.1016/j.jobe.2018.09.015.
[25] E. Quagliarini, S. Lenci, The influence of natural stabilizers and natural fibres on the mechanical properties of ancient Roman adobe bricks, Journal of Cultural Heritage. 11 (2010) 309–314. https://doi.org/10.1016/j.culher.2009.11.012.
[26] L. Aouba, M. Coutand, B. Perrin, H. Lemercier, Predicting thermal performance of fired clay bricks lightened by adding organic matter: Improvement of brick geometry, Journal of Building Physics. 38 (2015) 531–547. https://doi.org/10.1177/1744259115571078.
[27] L. Rincón, A. Carrobé, I. Martorell, M. Medrano, Improving thermal comfort of earthen dwellings in sub-Saharan Africa with passive design, Journal of Building Engineering. 24 (2019) 100732. https://doi.org/10.1016/j.jobe.2019.100732.
[28] J. Rojas, G. Barrios, G. Huelsz, R. Tovar, S. Jalife-Lozano, Thermal performance of two envelope systems: Measurements in non air-conditioned outdoor test cells and simulations, Journal of Building Physics. 39 (2016) 452–460. https://doi.org/10.1177/1744259115591993.

[29] F. Kuznik, J. Virgone, Experimental assessment of a phase change material for wall building use, Applied Energy. 86 (2009) 2038–2046. https://doi.org/10.1016/j.apenergy.2009.01.004.
[30] H. Manz, P. Loutzenhiser, T. Frank, P.A. Strachan, R. Bundi, G. Maxwell, Series of experiments for empirical validation of solar gain modeling in building energy simulation codes—Experimental setup, test cell characterization, specifications and uncertainty analysis, Building and Environment. 41 (2006) 1784–1797. https://doi.org/10.1016/j.buildenv.2005.07.020.
[31] P. Strachan, Model validation using the PASSYS Test cells, Building and Environment. 28 (1993) 153–165. https://doi.org/10.1016/0360-1323(93)90049-9.
[32] M. Gerber, EnergyPlus Energy Simulation Software, (2014).
[33] D.B. Crawley, EnergyPlus: DOE's Next Generation Simulation Program, Energy Efficiency and Renewable Energy, US Department of Energy. (2010).
[34] D.B. Crawley, L.K. Lawrie, C.O. Pedersen, F.C. Winkelmann, Energy plus: energy simulation program, ASHRAE Journal. 42 (2000) 49–56.
[35] D. Crawley, F. Winkelmann, L. Lawrie, C. Pedersen, EnergyPlus: a new-generation building energy simulation program, in: Forum-Proceedings, ASHRAE, 2001: pp. 575–580.
[36] J. Yang, H. Fu, M. Qin, Evaluation of Different Thermal Models in EnergyPlus for Calculating Moisture Effects on Building Energy Consumption in Different Climate Conditions, Procedia Engineering. 121 (2015) 1635–1641. https://doi.org/10.1016/j.proeng.2015.09.194.
[37] U.S. Department of Energy, EnergyPlus Engineering Reference, (2016).
[38] G.N. Walton, Thermal Analysis Research Program Reference Manual, National Bureau of Standards, March. (1983).
[39] ASHRAE, 2001 ASHRAE handbook: fundamentals., ASHRAE, Atlanta, GA., 2001.
[40] W.A.Y. Mousa, W. Lang, W.A. Yousef, Simulations and quantitative data analytic interpretations of indoor-outdoor temperatures in a high thermal mass structure, Journal of Building Engineering. 12 (2017) 68–76. https://doi.org/10.1016/j.jobe.2017.05.007.
[41] E. Stéphan, R. Cantin, A. Caucheteux, S. Tasca-Guernouti, P. Michel, Experimental assessment of thermal inertia in insulated and non-insulated old limestone buildings, Building and Environment. 80 (2014) 241–248. https://doi.org/10.1016/j.buildenv.2014.05.035.
[42] P. Strachan, K. Svehla, I. Heusler, M. Kersken, Whole model empirical validation on a full-scale building, Journal of Building Performance Simulation. 9 (2016) 331–350. https://doi.org/10.1080/19401493.2015.1064480.
[43] P.M. Toure, Y. Dieye, P.M. Gueye, V. Sambou, S. Bodian, S. Tiguampo, Experimental determination of time lag and decrement factor, Case Studies in Construction Materials. 11 (2019) e00298. https://doi.org/10.1016/j.cscm.2019.e00298.
[44] A. Moschella, A. Gagliano, A.L. Faro, A. Mondello, A. Salemi, G. Sanfilippo, A Methodology for an Integrated Approach for Seismic and Energy Refurbishment of Historic Buildings in Mediterranean Area, in: 2018. https://doi.org/10.3390/su10072448.
[45] H. Asan, Y.S. Sancaktar, Effects of Wall's thermophysical properties on time lag and decrement factor, Energy and Buildings. 28 (1998) 159–166. https://doi.org/10.1016/S0378-7788(98)00007-3.
[46] S. Shaik, A.B. Talanki Puttaranga Setty, Influence of ambient air relative humidity and temperature on thermal properties and unsteady thermal response characteristics of laterite wall houses, Building and Environment. 99 (2016) 170–183. https://doi.org/10.1016/j.buildenv.2016.01.030.